Antiphase boundaries in Hg_2Br_2 and KSCN

1993 J. Phys.: Condens. Matter 5 1455

(http://iopscience.iop.org/0953-8984/5/10/004)

J. Phys.: Condens. Matter 5 (1993) 1455–1472. Printed in the UK

Antiphase boundaries in Hg_2Br_2 and KSCN

I Rychetsky† and W Schranz
Institut für Experimentalphysik, Universität Wien, Strudlhofgasse 4, 1090-Wien, Austria

Received 24 September 1992, in final form 3 December 1992

Abstract. The angular dependences of the free energy, thickness and stresses are calculated for the antiphase boundaries (APBs) parallel to the tetragonal z axis but otherwise arbitrarily oriented. The general results are applied to Hg_2Br_2 and KSCN. The APB in the former case is shown to decay into two ferroelastic domain walls, while it is stable in KSCN. High stresses occur around the APB in KSCN and more than 50% of the free energy originates from the inhomogeneous strain in the wall. The observed etched patterns in KSCN are discussed.

1. *Introduction*

The orientations of coherent ferroelastic domain walls (FDWs) in ferroelastic crystals are fully determined by the different spontaneous deformations of both domains separated by the wall [1,2]. Even if the domains perfectly match at the coherent FDW, the gradually changing structure giving rise to the inhomogeneous strains results in the appearance of stresses in the FDW and an increase in the wall energy. In the framework of the Landau–Ginzburg phenomenological approach characteristics of the FDWs—the thickness and the surface energy—were studied in the perovskite crystal $BaTiO_3$ [3,4], which undergoes an improper ferroelastic proper ferroelectric phase transition. Recently a complex and consistent analysis of the domain walls in the improper ferroelastic perovskite crystal $SrTiO_3$ was performed [5,6]. It was shown that the usual assumption of the quasi-one-dimensional wall structure requires an appropriate distribution of the surface forces around the domain wall [5,6]. The known empirical values of the free-energy expansion coefficients for the $SrTiO_3$ crystal made the numerical estimation of the FDW characteristics possible.

Contrary to FDWs, the orientation of a non-ferroelastic domain wall (non-FDW) is not determined by the spontaneous deformation, since it is the same in both domains separated by the wall. Instead, the anisotropy of the crystal structure and the inhomogeneous strains in the wall [5] as well as the induced electric depolarization field [7] play an important role. The 180° ferroelectric domain wall in barium titanate [3] and the antiphase boundaries (APBs) in strontium titanate [5], which belong to the non-FDWs, were studied with respect to their crystallographic orientations. Their equilibrium structure was assumed to be linear (Ising type) and was described as a simple kink. The angle-dependent free energy and the thickness of the 180° ferroelectric domain walls were calculated for $BaTiO_3$ [8] and TGS [9].

† Permanent address: Institute of Physics, Czechoslovak Academy of Sciences, Na Slovance 2, 18040 Prague, Czechoslovakia.

0953-8984/93/101455+18$07.50

The results obtained were in qualitative agreement with the observed orientational anisotropy. Considering the deformations of the crystal in two dimensions only, the temperature-dependent orientation of the stress-free APB in the orthorhombic improper ferroelastics, e.g. $Gd_2(MoO_4)_3$, was calculated [10] and found to be in good agreement with experiments [11,12].

Several workers calculated the position-dependent order parameter in the domain wall, solving the Lagrange–Euler equations [13–20]. In particular, the stability of the linear structure of the APB, its transformation to the rotational structure and the corresponding phase diagram were worked out. This transformation to the rotational structure represents the nucleation of the orientational domain in the centre of the APB and the splitting of the APB into two FDWs.

In this paper the properties of the APBs in Hg_2Br_2 and KSCN are studied theoretically. The model and the general formulae for the angle-dependent free energy and for the thickness of the APB as well as the stress components are derived in sections 2–5. The results are applied to Hg_2Br_2 and KSCN in section 6 and section 7, respectively.

2. Free energy

We consider the free-energy density expansion appropriate to the description of the improper ferroelectric phase transitions in Hg_2Br_2 [21] and KSCN [29] driven by the two-component order parameter p, q. Up to the terms of the fourth order, one can write

$$f = f_0 + f_c + f_e + f_g \tag{1}$$

where

$$f_0 = \tfrac{1}{2}\alpha(p^2+q^2) + \tfrac{1}{4}\beta'(p^2-q^2)^2 + \tfrac{1}{2}\gamma' p^2 q^2 \qquad \alpha = \lambda(T - T_c) \tag{2a}$$

represents the free energy containing the primary order parameter only,

$$f_c = l_1'(p^2+q^2)(u_1+u_2) + l_6'(p^2-q^2)u_6 + l_3'(p^2+q^2)u_3 \tag{2b}$$

is the free energy of the coupling between the primary order parameter and the strain,

$$f_e = \tfrac{1}{2}[c_{11}(u_1^2+u_2^2) + c_{33}u_3^2 + c_{44}(u_4^2+u_5^2) + c_{66}u_6^2 + 2c_{12}u_1u_2 + 2c_{13}(u_1+u_2)u_3] \tag{2c}$$

is the elastic part of the free energy and

$$f_g = \tfrac{1}{2}g_1[(\partial_x p)^2 + (\partial_y p)^2 + (\partial_x q)^2 + (\partial_y q)^2] + \tfrac{1}{2}g_2(\partial_x p\,\partial_y p - \partial_x q\,\partial_y q) \tag{2d}$$

is the gradient term. The strain components u_i and the elastic constants c_{ij} are written in the Voigt notation: $xx = 1$, $yy = 2$, $zz = 3$, $yz = 4$, $xz = 5$, $xy = 6$. They are referred to the tetragonal coordinate system x, y, z shown in figure 1(*b*).

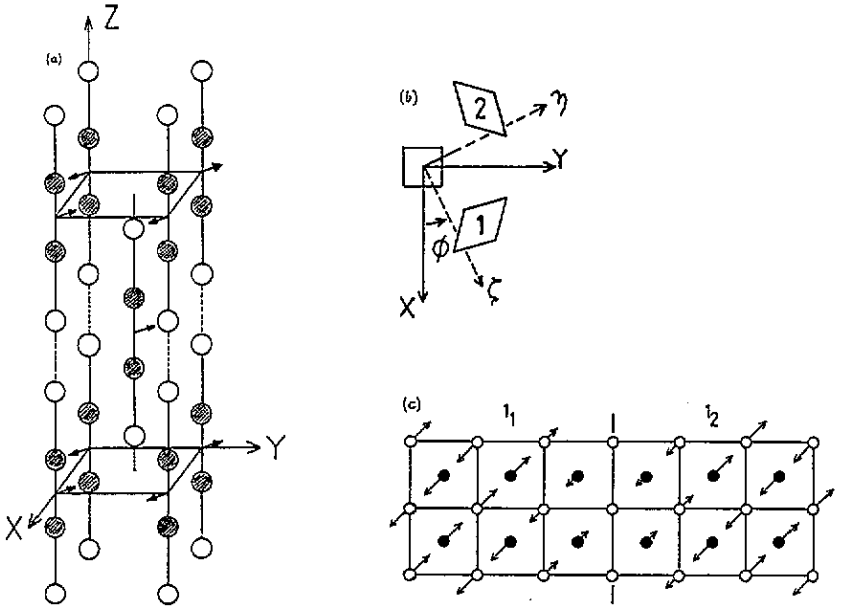

Figure 1. (*a*) Tetragonal unit cell of Hg_2Cl_2. (*b*) x, y are the tetragonal axes; ζ is the normal to the APB plane; η represents the APB plane. The shear strain of the ferroelastic domains 1 and 2 is also shown. (*c*) The microscopic structure of the [010] APB which is parallel to the FDW.

Since we shall study the walls parallel to the z axis but otherwise arbitrarily oriented, it is convenient to rewrite the strain tensor components and the elastic constants with respect to the coordinate system ζ, η, z (figure 1(*b*)), rotated through the angle ϕ around the z axis. The form of f_0 remains unchanged while the gradient terms, the coupling and the elastic free-energy terms are as follows:

$$f_g = \tfrac{1}{2}g_+[(\partial_\zeta p)^2 + (\partial_\eta q)^2] + \tfrac{1}{2}g_-[(\partial_\eta p)^2 + (\partial_\zeta q)^2] \tag{2d'}$$

where $g_+ = g_i + g_a \sin(2\phi)$ and $g_- = g_i - g_a \sin(2\phi)$;

$$f_c = (l'_+ p^2 + l'_- q^2)u'_1 + (l'_- p^2 + l'_+ q^2)u'_2 + l'_6 \cos(2\phi)\,(p^2 - q^2)u'_6 + l'_3(p^2 + q^2)u'_3 \tag{2b'}$$

where $l_\pm = l'_1 \pm l'_6 \sin(2\phi)$;

$$f_e = \tfrac{1}{2}[A_{11}(u'^2_1 + u'^2_2) + A_{33}u'^2_3 + A_{44}(u'^2_4 + u'^2_5) + A_{66}u'^2_6 + 2A_{12}u'_1u'_2 + 2A_{13}(u'_1 + u'_2)u'_3 + 2A_{16}u'_6(u'_2 - u'_1)]. \tag{2c'}$$

The elastic constants A_{ij} and the strain components u'_i are now written in the Voigt notation, referred to the ζ, η and z axes, i.e. $\zeta\zeta = 1$, $\eta\eta = 2$, $zz = 3$, $\eta z = 4$,

$\zeta z = 5$, $\zeta \eta = 6$. The matrix of the elastic constants has the form

$$A_{ij} = \begin{bmatrix} A_{11} & A_{12} & A_{13} & 0 & 0 & -A_{16} \\ A_{12} & A_{11} & A_{13} & 0 & 0 & A_{16} \\ A_{13} & A_{13} & A_{33} & 0 & 0 & 0 \\ 0 & 0 & 0 & A_{44} & 0 & 0 \\ 0 & 0 & 0 & 0 & A_{44} & 0 \\ -A_{16} & A_{16} & 0 & 0 & 0 & A_{66} \end{bmatrix}$$

with

$$\begin{aligned} A_{11} &= \tfrac{1}{4}[(c_{11} - c_{12} - 2c_{66})\cos(4\phi) + 3c_{11} + c_{12} + 2c_{66}] \\ A_{12} &= \tfrac{1}{4}[(c_{12} - c_{11} + 2c_{66})\cos(4\phi) + 3c_{12} + c_{11} - 2c_{66}] \\ A_{66} &= \tfrac{1}{4}[(c_{12} - c_{11} + 2c_{66})\cos(4\phi) + c_{11} - c_{12} + 2c_{66}] \\ A_{16} &= \tfrac{1}{4}(c_{11} - c_{12} - 2c_{66})\sin(4\phi) \\ A_{44} &= c_{44} \qquad A_{33} = c_{33} \qquad A_{13} = c_{13}. \end{aligned} \tag{3}$$

For use in the following we write the formula of the determinant Δ of the 4×4 matrix, obtained by skipping the fourth and the fifth rows and columns in A_{ij}:

$$\begin{aligned} \Delta &= [A_{66}(A_{11} - A_{12}) - 2A_{16}^2][A_{33}(A_{11} + A_{12}) - 2A_{13}^2] \\ &= c_{66}(c_{11} - c_{12})[c_{33}(c_{11} + c_{12}) - 2c_{13}^2] \end{aligned} \tag{4}$$

and the determinant Δ' of the 2×2 matrix, when skipping rows and columns with numbers 2, 3, 4 and 5:

$$\Delta' = A_{11}A_{66} - A_{16}^2 = c_{11}c_{66} + \tfrac{1}{4}(c_{11} + c_{12})(c_{11} - c_{12} - 2c_{66})\sin^2(2\phi). \tag{5}$$

3. Equilibrium conditions

We shall study a quasi-one-dimensional wall parallel to the η–z plane and perpendicular to the ζ axis. The wall is represented by the η axis in figure 1(*b*), its orientation is characterized by the single angle ϕ and all quantities depend on the coordinate ζ only. Such a quasi-one-dimensional system is an example of a layered structure, and the equilibrium conditions [5] can be written in the simplified form [22]

$$(\partial/\partial\zeta)(\partial f/\partial p_\zeta) - \partial f/\partial p = 0 \tag{6a}$$

$$(\partial/\partial\zeta)(\partial f/\partial q_\zeta) - \partial f/\partial q = 0 \tag{6b}$$

$$\sigma_1' = \sigma_5' = \sigma_6' = 0. \tag{6c}$$

The stress components σ_i', referred to the ζ, η, z coordinate system, are

$$\sigma_i' = \partial f/\partial u_i' \qquad i = 1, \ldots, 6. \tag{7}$$

The stresses σ_2', σ_3' and σ_4' are in principle non-zero and can be calculated from equation (7). The non-zero stress components are the consequences of the compatibility conditions of the strain, which must be fulfilled in a defectless crystal. In our layered system the deformations u_2', u_3' and u_4' should be constant over all the space [22]:

$$u_2'(\zeta) = u_2'(\infty) \qquad u_3'(\zeta) = u_3'(\infty) \qquad u_4'(\zeta) = u_4'(\infty). \tag{8}$$

Equations (6*c*) claim that the system can relax along the ζ direction until the stresses σ_1', σ_5' and σ_6' are zero. Simultaneously, in order to keep the strains u_2', u_3' and u_4' in the η–z planes constant (independent of their positions ζ) according to equations (8), the non-zero stresses σ_2', σ_3' and σ_4' must be imposed at the crystal surface.

4. Homogeneous phase

In the homogoneous crystal all stresses are zero and the system of equations (6)–(8) gives the spontaneous homogeneous deformations

$$\begin{aligned}
&u_{1s} = l_1(p_s^2 + q_s^2) \qquad && l_1 = -(1/\Delta)(l_1'c_{33} - l_3'c_{13})(c_{11} - c_{12})c_{66} \\
&u_{2s} = u_{1s} \\
&u_{3s} = l_3(p_s^2 + q_s^2) \qquad && l_3 = -(1/\Delta)[l_3'(c_{11} + c_{12}) - 2l_1'c_{13}](c_{11} - c_{12})c_{66} \\
&u_{6s} = l_6(p_s^2 - q_s^2) \qquad && l_6 = -l_6'/c_{66} \\
&u_{4s} = u_{5s} = 0
\end{aligned} \tag{9}$$

where the spontaneous values p_s and q_s minimize the reduced free energy

$$f = \tfrac{1}{2}\alpha(p^2 + q^2) + \tfrac{1}{4}\beta(p^4 + q^4) + \tfrac{1}{2}\gamma p^2 q^2 \tag{10a}$$

with

$$\beta = \beta' - 4\Lambda \tag{10b}$$

$$\gamma = \gamma' - \beta' - 4(\Lambda - l_6'^2/c_{66}) \tag{10c}$$

and

$$\Lambda = l_1'^2(s_{11} + s_{12}) + 2l_1'l_3's_{13} + l_3'^2 s_{33}/2 + l_6'^2 s_{66}/2. \tag{10d}$$

The reduced free energy (10*a*) was derived from equation (1) eliminating the strains by means of equations (7).

Below T_c, $t < 0$, and assuming that

$$\gamma > \beta > 0 \tag{11}$$

the four stable domain states are

$$\begin{aligned} 1_1 &: p_s = -p_0 \qquad q_s = 0 \\ 1_2 &: p_s = +p_0 \qquad q_s = 0 \end{aligned} \qquad u_{6s} = -l_6 p_0^2 \tag{12a}$$

$$\begin{aligned} 2_1 &: p_s = 0 \qquad q_s = +p_0 \\ 2_2 &: p_s = 0 \qquad q_s = -p_0 \end{aligned} \qquad u_{6s} = +l_6 p_0^2 \tag{12b}$$

where $p_0 = \sqrt{-\alpha/\beta}$. The spontaneous shear strain u_{6s} in (12) indicates the macroscopic difference between the ferroelastic domain states 1 and 2. The structures corresponding to the domain states with equal shear (e.g. equation (12*a*)) are mutually shifted by a primitive vector [21,30] of the high-symmetry phase and distinguished by the subscript. The free-energy density of the low-temperature phase equals

$$F_0 = -\alpha^2/4\beta. \tag{13}$$

5. Antiphase boundary

Let us consider the APB perpendicular to the ζ axis and separating domains 1_1 and 1_2. Then the system of equations (6)–(8) is to be solved with the boundary conditions

$$\begin{aligned} p(\zeta = +\infty) &= -p(\zeta = -\infty) = p_0 \\ q(\zeta = +\infty) &= q(\zeta = -\infty) = 0. \end{aligned} \tag{14}$$

Far away from the domain wall the crystal is homogeneous and possesses the spontaneous strains u_{is}, i.e. $u_i(\infty) = u_{is}$. The position-independent strains (8) are

$$\begin{aligned} u_2'(\zeta) = u_{2s}' &= \Delta^{-1}\{(l_1' A_{33} - l_3' A_{13})[2A_{16}^2 - A_{66}(A_{11} - A_{12})] \\ &\quad + l_6'[A_{33}(A_{11} + A_{12}) - 2A_{13}^2][A_{66}\sin(2\phi) + A_{16}\cos(2\phi)]\}p_0^2 \\ u_3'(\zeta) = u_{3s}' &= \Delta^{-1}[-2l_1' A_{13} + l_3'(A_{11} + A_{12})][2A_{16}^2 - A_{66}(A_{11} - A_{12})]p_0^2 \\ u_4'(\zeta) = u_{4s}' &= 0. \end{aligned} \tag{15}$$

The spontaneous values (15) can be calculated from (9) using the rotated axes ζ, η and z, or directly from the free energy (1) with its terms written with respect to the rotated system. The remaining position-dependent strain components, as derived from equations (6c), (7) and (1), take the form

$$\begin{aligned} u_1'(\zeta) &= -\Delta'^{-1}[\{l_1' A_{66} + l_6'[A_{66}\sin(2\phi) + A_{16}\cos(2\phi)]\}p(\zeta)^2 \\ &\quad + \{l_1' A_{66} - l_6'[A_{66}\sin(2\phi) + A_{16}\cos(2\phi)]\}q(\zeta)^2 \\ &\quad + (A_{66}A_{12} + A_{16}^2)u_2' + A_{66}A_{13}u_3'] \\ u_6'(\zeta) &= -\Delta'^{-1}[\{l_1' A_{16} + l_6'[A_{16}\sin(2\phi) + A_{11}\cos(2\phi)]\}p(\zeta)^2 \\ &\quad + \{l_1' A_{16} - l_6'[A_{16}\sin(2\phi) + A_{11}\cos(2\phi)]\}q(\zeta)^2 \\ &\quad + A_{16}(A_{12} + A_{11})u_2' + A_{16}A_{13}u_3'] \\ u_5'(\zeta) &= 0. \end{aligned} \tag{16}$$

Using (7) and taking into account (15) and (16) the formulae for the non-zero and position-dependent stresses read

$$\sigma_2'(\zeta) = [p(\zeta)^2 - p_0^2][b_{21} + b_{22}\sin(2\phi)]/\Delta' + q(\zeta)^2[b_{21} - b_{22}\sin(2\phi)]/\Delta'$$
$$\sigma_3'(\zeta) = [p(\zeta)^2 - p_0^2][l_3'\Delta' + b_{31} + b_{32}\sin(2\phi) + b_{33}\sin^2(2\phi)/\Delta'$$
$$+ q(\zeta)^2[l_3'\Delta' + b_{31} - b_{32}\sin(2\phi) + b_{33}\sin^2(2\phi)/\Delta'$$
$$\sigma_4'(\zeta) = 0 \tag{17a}$$

where

$$b_{21} = l_1'c_{66}(c_{11} - c_{12}) \qquad b_{22} = -l_6'(c_{11} + c_{12})(c_{11} - c_{12})/2$$
$$b_{31} = -l_1'c_{13}c_{66} \tag{17b}$$
$$b_{32} = -l_6'c_{13}(c_{11} - c_{12})/2 \qquad b_{33} = -l_1'c_{13}(c_{11} - c_{12} - 2c_{66})/2.$$

The position-dependent order parameter $p(\zeta)$, $q(\zeta)$ occurring in (16) and (17) is still not determined. For this purpose we eliminate the strains u_i' making use of (15) and (16) from the free energy (1) and finally obtain the reduced free energy

$$f = \tfrac{1}{2}(\alpha_p p^2 + \alpha_q q^2) + \tfrac{1}{4}(\beta_p p^4 + \beta_q q^4) + \tfrac{1}{2}\gamma^* p^2 q^2 + \tfrac{1}{2}[g_+(\partial_\zeta p)^2 + g_-(\partial_\zeta q)^2] \tag{18a}$$

where we took into account the order parameter is independent of the η axis. The coefficients in (18*a*) read

$$\alpha_p = t + 2p_0^2[-2\Lambda\Delta' + k_1 + k_2\sin(2\phi) + k_3\sin^2(2\phi)]/\Delta'$$
$$\alpha_q = t + 2p_0^2[-2\Lambda\Delta' + k_1 + k_3\sin^2(2\phi)]/\Delta'$$
$$\beta_p = \beta' - 2[k_1 + k_2\sin(2\phi) + k_3\sin^2(2\phi)/\Delta' \tag{18b}$$
$$\beta_q = \beta' - 2[k_1 - k_2\sin(2\phi) + k_3\sin^2(2\phi)]/\Delta'$$
$$\gamma^* = \gamma' - \beta' - 2[k_1' + k_3'\sin^2(2\phi)]/\Delta'$$

where

$$k_1 = l_1'^2c_{66} + l_6'^2c_{11} \qquad k_1' = l_1'^2c_{66} - l_6'^2c_{11} \qquad k_2 = l_1'l_6'(c_{11} - c_{12})$$
$$k_3 = [l_1'^2(c_{11} - c_{12} - 2c_{66}) - l_6'^2(c_{11} + c_{12})]/2 \tag{18c}$$
$$k_3' = [l_1'^2(c_{11} - c_{12} - 2c_{66}) + l_6'^2(c_{11} + c_{12})]/2.$$

The Lagrange–Euler equations (6*a*) and (6*b*) with the reduced free energy (18*a*) are

$$g_+\,\partial_{\zeta\zeta}^2 p = \alpha_p p + \beta_p p^3 + \gamma^* p q^2$$
$$g_-\,\partial_{\zeta\zeta}^2 q = \alpha_q q + \beta_q q^3 + \gamma^* q p^2. \tag{19}$$

Summarizing, the orientation of the APB, perpendicular to ζ, is described by the angle ϕ. The position-dependent order parameter in the boundary is represented by the solution of the differential equations (19) with the boundary conditions (14). The stresses and deformations in the APB are given by (15), (16), (17*a*) and (6*c*).

Taking into account the equality

$$\alpha_p/\beta_p = \alpha/\beta \tag{20}$$

the simple kink solution of equations (19) and (16) exists:

$$\begin{aligned} p(\zeta) &= p_0 \tanh(2\zeta/d_{\mathrm{APB}}) \\ q(\zeta) &= 0 \end{aligned} \tag{21}$$

where

$$d_{\mathrm{APB}} = 2[(-\alpha/2g_+\beta)\beta_p]^{-1/2}. \tag{22}$$

The thickness d_{APB} of the APB depends on the angle ϕ. The substitution of (21) into (18*a*) leads to the formula for the angle-dependent surface free energy:

$$\sigma_{\mathrm{APB}} = \int_{-\infty}^{+\infty} [f(\zeta) - f_0]\,\mathrm{d}\zeta = \tfrac{4}{3}|F_0|d_{\mathrm{APB}}\beta_p/\beta. \tag{23}$$

We shall further consider $g_s = 0$ in accord with the assumptions made for Hg_2Br_2 and KSCN in sections 6 and 7. Differentiating (23) with respect to the angle ϕ we obtain the equation determining the extremes of σ_{APB}:

$$[\sin(2\phi) - A][\sin(2\phi) - B]\cos(2\phi) = 0 \tag{24a}$$

where

$$A = 2l_1'c_{66}/l_6'(c_{11} + c_{12}) \qquad B = [-4c_{11}c_{66}/(c_{11} + c_{12})(c_{11} - c_{12} - 2c_{66})](1/A). \tag{24b}$$

In the following analysis we assume that $l_1' > 0$ and $l_6' > 0$. The condition of the positive definite elastic free energy (2*c*) requires the non-zero elastic constants c_{ij}, $i, j = 1, \ldots, 6$, to be positive and $c_{11} - c_{12} > 0$. If we make use of this, the analysis of the extremes given by equation (24*a*) yields the results shown in tables 1 and 2. Note that $B < 0$ for $c_{11} - c_{12} - 2c_{66} > 0$ (table 1) and $B > 0$ for $c_{11} - c_{12} - 2c_{66} < 0$ (table 2). If $0 < A < 1$ (see tables 1 and 2), then there exist two minima $\phi_\pm = \frac{1}{4}\pi \pm (\frac{1}{2}\sin^{-1} A - \frac{1}{4}\pi)$ and the uniaxial stress σ_2', which is parallel to the APB plane, is zero over all the space. A similar result, except for a factor of 2, was obtained earlier [10] considering the two-dimensional deformations. If moreover $0 > B > -1$ (table 1), an additional metastable minimum at $-\frac{1}{4}\pi$ appears.

For $A > 1$ and $B < 0$ (table 1) the single absolute minimum of σ_{APB} at the crystallographic value $\phi_\pm = \frac{1}{4}\pi$ exists. For this angle the stress σ_2' given by equation (17*a*) possesses its lowest, but non-zero absolute value.

For $A > 1$ and $B > 0$, two cases can occur. If $B > 1$ (table 2) the free energy has its lowest value at $\phi_\pm = \frac{1}{4}\pi$. If $0 < B < 1$, the two degenerate

Table 1. $c_{11} - c_{12} - c_{66}/2 > 0$ ($B < 0$). ami = absolute minimum; mmi = metastable minimum; max = maximum.

	$0 < A < 1$			$A > 1$	
ami	$\phi_\pm = \pi/4 \pm (\frac{1}{2}\arcsin A - \pi/4)$		$\sigma_2' = 0$	$\phi_\pm = \pi/4$	$\sigma_2' \neq 0$
	$B < -1$	$0 > B > -1$		$B < -1$	$0 > B > -1$
mmi	—	$-\pi/4$		—	$-\pi/4$
max	$-\pi/4$; $+\pi/4$	$-\pi/4 \pm (\frac{1}{2}\arcsin B + \pi/4)$; $-\pi/4$		$-\pi/4$	$-\pi/4 \pm (\frac{1}{2}\arcsin B + \pi/4)$

Table 2. $c_{11} - c_{12} - c_{66}/2 < 0$ ($B > 0$). In the interval $2 - 1/A > B$ (> 0) schematically shown in the last row, the lowest magnitude of σ_2' does not correspond to the minimum free energy.

	$0 < A < 1$	$A > 1$	
	$B > 1$	$B > 1$	$1 > B > 0$
ami	$\phi_\pm = \pi/4 \pm (\frac{1}{2}\arcsin A - \pi/4)$	$\phi_\pm = \pi/4$	$\phi_\pm = \pi/4 \pm (\frac{1}{2}\arcsin B - \pi/4)$
	$\sigma_2' = 0$	$\sigma_2' \neq 0$	$\sigma_2' \neq 0$
max	$-\pi/4$ and $+\pi/4$	$-\pi/4$	$-\pi/4$ and $+\pi/4$
		$B > 2 - 1/A$	$2 - 1/A > B$

minima of the free energy at $\phi_\pm = \frac{1}{4}\pi \pm (\frac{1}{2}\sin^{-1} B - \frac{1}{4}\pi)$ appear. The stress σ_2' is non-zero in the whole interval $A > 1$, $B > 0$. Nevertheless, analysing equation (17*a*) one can find that the lowest magnitude of σ_2' occurs at the angle $\phi_\pm = \frac{1}{4}\pi$ (i.e. at the angle of the minimum σ_{APB}) for $B > 2 - 1/A\,(> 1)$. For $2 - 1/A > B\,(> 0)$ the magnitude of the component σ_2' becomes lowest at the angles $\overline{\phi}_\pm = \frac{1}{4}\pi \pm \{\frac{1}{2}\sin^{-1}[A(1 - \sqrt{1 - B/A})] - \frac{1}{4}\pi\}$, which do not correspond to the minimum free energy.

It is worthwhile pointing out that the only z-dependent quantity is σ_3' (equation (17*a*)), while the remaining expressions σ_2' and (18*a*)–(24*b*) involve the x–y plane only. This means that by imposing the appropriate stress σ_3' along the z axis we effectively deal with two-dimensional deformations. The inhomogeneous stresses σ_2' and σ_3' must be imposed around the APB plane to sustain the quasi-one-dimensional structure [5,6] of the wall.

The temperature-dependent coefficients l_1' and l_6' result in the temperature dependence of the APB orientation. They were proposed to originate from the higher-order terms of the free-energy expansion [10]. On the assumption of an increase in A from 0 to 1 with increasing temperature [10], the two minima ϕ_+ and ϕ_- gradually approach $\frac{1}{4}\pi$. When $A > 1$ and $B > 1$, the APB is locked at the crystallographic orientation $\frac{1}{4}\pi$. Nevertheless, for $c_{11} - c_{12} - c_{66}/2 < 0$ (table 2) a further increase in A decreases B (24*b*) until $B < 1$. In this region, contrary to the assumption in [10], the APB is no longer locked at the angle $\frac{1}{4}\pi$, but two degenerate minima of the free energy with non-zero σ_2' appear at ϕ_+ and ϕ_-.

So far we have studied the linear APB (21), which is not always stable. If we make use of the result of Bullbich and Gufan [20], the linear structure (21) is unstable, when

$$h(\phi) = (\alpha_q/\alpha_p)\left\{4g/[(1+8g\gamma^*/\beta_p)^{1/2}-1]\right\} - 1 > 0 \qquad (25)$$

where $g = g_+/g_-$. Then the linear structure transforms into the rotational structure characterized by the non-zero order parameter component q in the APB centre. The rotational structure corresponds to the nucleation of the ferroelastic domain 2_1 (or 2_2) with the shear strain $u_6 = +l_6 q_c^2$, where q_c is the value of the order parameter component q in the centre of the APB (see (12*b*)). In our case, where the free energy has been expanded up to the fourth order, the instability of the linear structure leads to complete splitting of the APB into two FDWs [19].

6. Antiphase boundary in Hg_2Br_2

The tetragonal high-temperature phase (space group, $D_{4h}^{17}(I4/mmm)$) of Hg_2Br_2 is built up from the linear Br–Hg–Hg–Br molecules arranged in chains, which are parallel to the z axis. Such a body-centred structure is strongly anisotropic (figure 1(*a*)). The phase transition [21] at 143 K to the orthorhombic phase (space group, $D_{2h}^{17}(Cmcm)$) is induced by the transverse acoustic soft modes at the two non-equivalent X points of the Brillouin zone: $X_1 \equiv (\frac{1}{2}a, \frac{1}{2}a, 0)$ and $X_2 \equiv (\frac{1}{2}a, -\frac{1}{2}a, 0)$. It is accompanied by the antiferrodistortive displacements of the mass centres of molecules in the [110] and [1$\bar{1}$0] directions (figure 1). The linear APB structure is schematically shown in figure 1(*c*) for the (010) APB plane ($\phi = 90°$) [25]. The coefficients of the free energy (1) were deduced from the acoustic measurements [23], and from the temperature dependence of the soft-mode frequency and the linear thermal expansion coefficients [24] (table 3). The coupling constant g_i was estimated as [23] $g_i^3 \simeq (g_i^2 - g_a^2)g_{zz}$, where g_{zz} represents the coefficient of the gradient term along the z direction and g_a was assumed to be zero. The elastic constants determined by acoustic measurements [26] are

$$c_{11} = 16.6\,\text{GPa} \qquad c_{12} = 15.00\,\text{GPa} \qquad c_{13} = 18.88\,\text{GPa}$$
$$c_{33} = 88.85\,\text{GPa} \qquad c_{66} = 11.19\,\text{GPa} \qquad c_{44} = 7.446\,\text{GPa}.$$

With these values, $0 < A < 1$ and $B < -1$ (table 1). The APB with the minimum free energy is oriented at the angles $\phi_- = 15.4°$ and $\phi_+ = 90° - 15.4° = 74.6°$, which are close to the angles of the FDWs (100) ($\phi = 0°$) and (010) ($\phi = 90°$). The values ϕ_+ and ϕ_- represent the only orientations at which the stress component σ_2' is equal to zero. The angular dependences of the surface free energy σ_{APB} and the APB thickness d_{APB} are shown in figure 2 for $T_c - T = 5$ K. The position-dependent stress components $\sigma_2'(\zeta)$ and $\sigma_3'(\zeta)$ at the angles $-45°$, $45°$ and $\phi_\pm$ (extremes of the free energy) are plotted in figures 3(*a*) and 3(*b*), respectively. The angular dependence of the stresses $\sigma_2'(0)$ and $\sigma_3'(0)$ at the centre of the APB are plotted in figure 4. The free energies, the APB thicknesses and the stresses at the angles of the free-energy extremes are given in table 4. The thickness d_{APB} changes with the angle from 70 lattice constants at $\phi_\pm$ to 40 lattice constants at $-45°$. Since the function $h(\phi)$ in equation (25) is positive for all angles, the linear APB structure is always unstable. In spite of this the above analysis of the linear structure gives us an analytically tractable example of the APB, and its characteristics can be compared with the boundaries in other crystals, particularly in KSCN discussed in section 7.

It should be mentioned that the stability of the linear structure depends [27] on the value of the coupling coefficient $(\gamma'-\beta')/2$ between the order parameter components p and q (see equation (2*a*)). For the other physical properties of the linear APB this coupling is irrelevant.

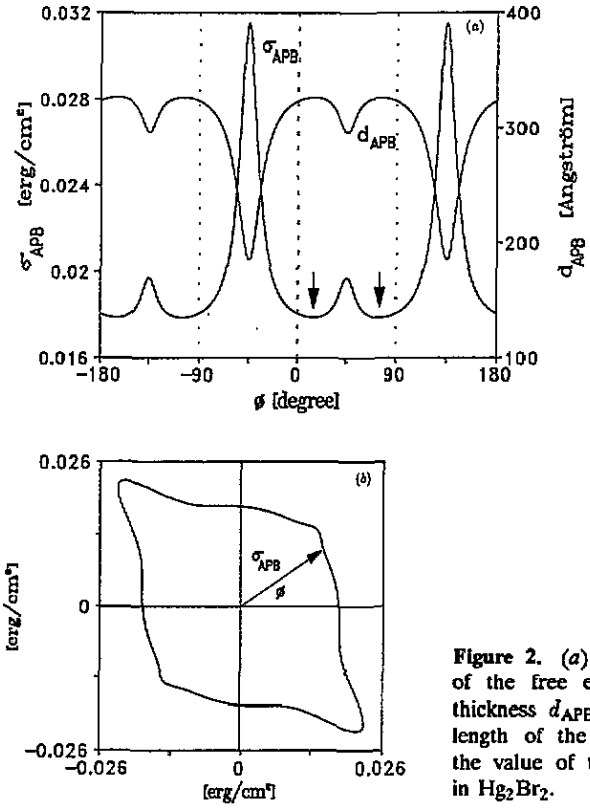

Figure 2. (*a*) The angular dependence of the free energy $\sigma_{APB}(\phi)$ and the thickness $d_{APB}(\phi)$ in Hg_2Br_2. (*b*) The length of the radius vector represents the value of the free energy $\sigma_{APB}(\phi)$ in Hg_2Br_2.

Table 3. Coefficients of the free energy for Hg_2Br_2 (*a*) values according to Lemanov *et al* [23], (*b*) values according to Barta *et al* [24].

(*a*)	$l_1^{\prime 2}/\beta'$ (J m^{-3})	$l_3^{\prime 2}/\beta'$ (J m^{-3})	$l_6^{\prime 2}/\beta'$ (J m^{-3})	$2(\gamma'-\beta')/\beta'$ —	$\beta'/\sqrt{(\lambda g_i^3)}$ (K$^{1/2}$ J^{-1})
	1.43×10^9	2.5×10^9	2.8×10^9	~ 1	2.8×10^{21}
(*b*)	$\beta' V$ (J)	λV (J K^{-1})	V (m^{-3})	$g_i V$ (J m^2)	
	2.006×10^{15}	22.3×10^{-7}	120×10^{-30}	1.49×10^{-21}	

It is also interesting to estimate the share of the free energy arising from the inhomogeneous strain. If the APB is cut into thin slices perpendicular to the ζ

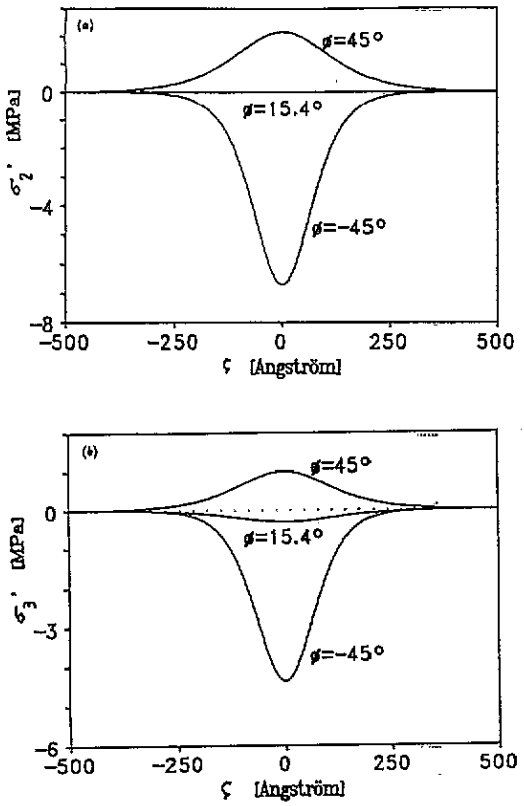

Figure 3. (*a*) The position-dependent stress component $\sigma_2'(\zeta)$ for three angles corresponding to extremal values of the free energy in Hg_2Br_2. (*b*) The position-dependent stress component $\sigma_3'(\zeta)$ for three angles corresponding to extremal values of the free energy in Hg_2Br_2.

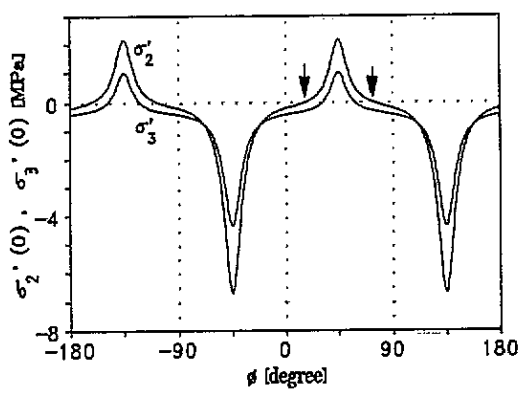

Figure 4. The stress components $\sigma_2'(0)$ and $\sigma_3'(0)$ in the centre of the APB versus the angle ϕ. The APB with the minimum free energy possesses the zero σ_2' component (shown by arrows).

axis and each of them are allowed to deform freely (i.e. neighbouring layers need not match each other and the compatability conditions (8) are not operating), the homogeneous part of the free energy (18*a*) should be replaced with (10*a*). The value of the free energy is then 0.01784 erg cm^{-2}. Consequently, for the orientation $\phi_{\pm}$, around 0% (less than 0.005%) of the free energy has a mechanical origin, while it is 42% for the angle $-\frac{1}{4}\pi$.

Table 4. The free energies, APB thicknesses and the stresses at several angles.

Angle (deg)	σ_{APB} (erg cm^{-2})	$\sigma_2'(0)$ (MPa)	$\sigma_3'(0)$ (MPa)	d_{APB} (Å)
$\phi_\pm$	0.01785	0.0	−0.3	327
45	0.020	2.2	1.0	296
−45	0.031	−6.7	−4.4	185

7. Antiphase boundaries in KSCN

The KSCN crystal has a body-centred tetragonal structure of the high-temperature phase with the space group $D_{4h}^{18}(I4/mcm)$ and two molecules in the unit cell. The structure is built up from layers which are perpendicular to the z axis. These layers contain the orientationally disordered SCN^- dipoles (lying in the layers) and alternate with layers of K^+ ions. The phase transition at 414 K is connected with the head–tail antiparallel ordering of SCN^- dipoles [28], resulting in a doubling of the primitive cell and a reduction in the symmetry to the $D_{2h}^{11}(Pbcm)$ space group [29]. The tetragonal structure is depicted in figure 5(*b*) and the linear APB is schematically shown [30] in figure 5(*c*). In the x, y coordinate system, which is rotated through 45° with respect to the tetragonal x', y' axis used in other papers [29–31], the results in section 5 are directly applicable. The elastic constants calculated from the ultrasonic measurements are [33]

$$c_{11} = 25.70\,\text{GPa} \qquad c_{12} = 18.70\,\text{GPa} \qquad c_{13} = 2.50\,\text{GPa}$$

$$c_{33} = 19.00\,\text{GPa} \qquad c_{66} = 31.20\,\text{GPa} \qquad c_{44} = 4.00\,\text{GPa}.$$

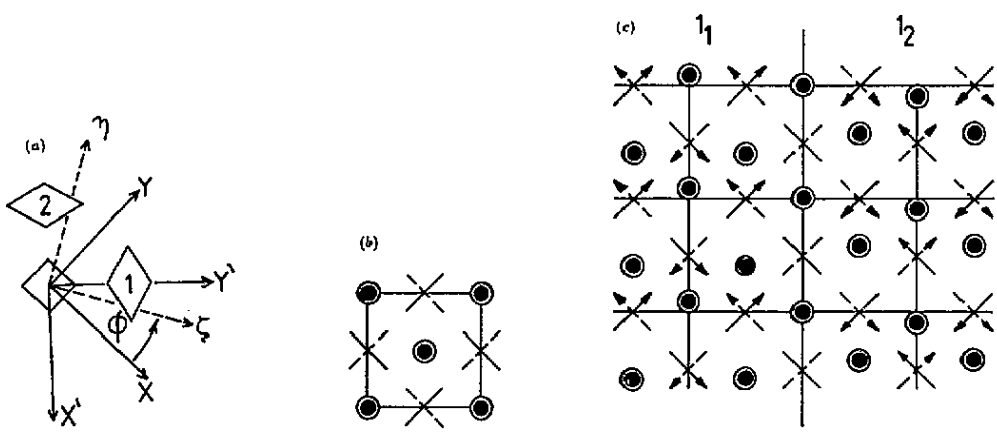

Figure 5. (*a*) x', y' are the natural tetragonal axes of KSCN; x, y are the tetragonal axes used in this paper; ζ is the normal to the APB plane. The spontaneous shear strain is also shown. (*b*) The tetragonal unit cell of KSCN. The open and full circles represent K^+ ions; the full and broken lines represent SCN^- groups. (*c*) The structure of the [110] (referred to x, y axes) APB, which makes an angle of 45° with the FDW.

The coefficients of the free energy (1) (table 5) can be estimated within the compressible pseudo-spin model [32], expanding the mean-field free energy up to the fourth order. The coefficients l_1', l_6', l_3' and β' were calculated using the results of the acoustic measurements [33]. For the value of λ the formula $\lambda = 4k_B/V$ has been used, where k_B is the Boltzmann constant and V is the volume of the orthorhombic cell [32]. The coefficient g_i of the gradient term was determined from the correlation length measured by diffuse neutron scattering [34] and the coefficient g_a was assumed to be zero. The expansion coefficients are collected in table 5.

Table 5. The free energy expansion coefficients of KSCN.

l_1' (MPa)	l_3' (MPa)	l_6' (MPa)	λ (MPa K^{-1})	β' (MPa)	γ' (MPa)	g_i (J m^{-1})
193.31	255.75	−84.24	0.08	11.23	$4\beta'$	1.76×10^{-9}

In the following we consider $T = T_c - 5$ K at which $p_0 = 0.46$. Note that the magnitude of the stresses (17*a*) is proportional to the value p_0^2. The angular dependences of the free energy σ_{APB} and the wall thickness d_{APB} are plotted in figure 6. The position-dependent stress components $\sigma_2'(\zeta)$ and $\sigma_3'(\zeta)$ at the angles −45°, 45° and $\phi_\pm$ are shown in figures 7(*a*) and 7(*b*), respectively, and the stresses $\sigma_2'(0)$ and $\sigma_3'(0)$ at the boundary centre versus the angle ϕ are depicted in figure 8. The values of the free energy, the APB thickness and stresses at several angles are (see the text below) given in table 6.

Table 6. Free energies, APB thicknesses and stresses at several angles.

Angle (deg)	σ_{APB} (erg cm^{-2})	$\sigma_2'(0)$ (MPa)	$\sigma_3'(0)$ (MPa)	d_{APB} (Å)
$\phi_\pm$	0.4642	−13.7	−61.71	26.3
$\bar{\phi}_\pm$	0.4646	−13.3	−61.69	26.2
45	0.48	−40.6	−63.2	25.4
−45	0.55	−77.1	−65.3	22.4

Since $A > 1$ and $0 < B < 1$ (table 2) the APB with the lowest free energy can have two orientations $\phi_+ = 11.9°$ and $\phi_- = 78.1°$, while the orientations with the lowest magnitude of the stress σ_2' are $\bar{\phi}_+ = 6.0°$ and $\bar{\phi}_- = 84.0°$. The anisotropy of the free energy is lower than for Hg_2Br_2, but its value is more than ten times higher (figures 2 and 6). From figure 6(*a*), one can also expect the APB orientation to be symmetrically distributed around 45°, while the angles from the interval (−90°, 0°) correspond to the higher values of the free energy. This agrees with the dominant 45° direction observed in the etched pattern [31,35]. The stress σ_2' varies with the angle from 13 to 77 MPa, not going to zero. The component σ_3' varies only slightly from 62 to 65 MPa (figure 8; see for comparison figure 4). The APB is strongly strained. One can estimate the part of the free energy corresponding to inhomogeneous deformations in a similar way to Hg_2Br_2. For the angles $\phi_\pm$, 55%

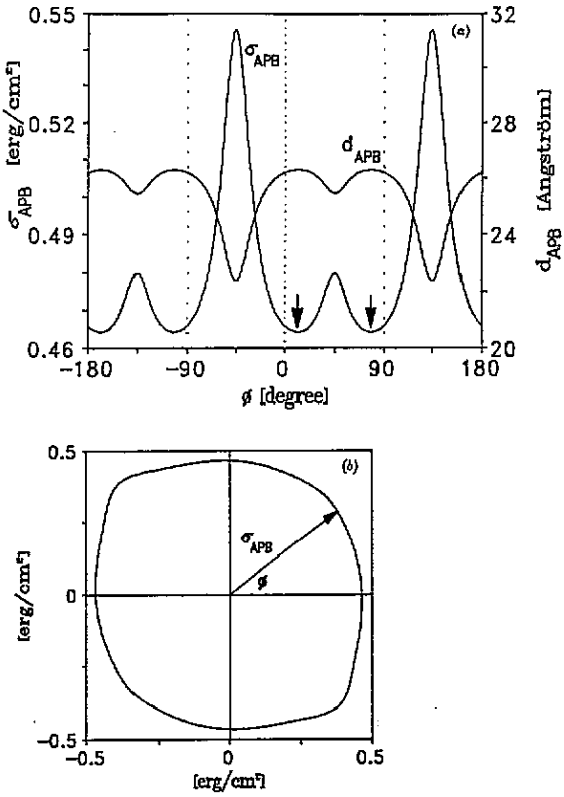

Figure 6. (*a*) The angular dependence of the free energy $\sigma_{APB}(\phi)$ and the thickness $d_{APB}(\phi)$ in KSCN. (*b*) The length of the radius vector represents the value of the free energy $\sigma_{APB}(\phi)$ in KSCN.

of the total free energy has a mechanical origin. For $\phi = -\frac{1}{4}\pi$ the corresponding percentage is 62%. The thickness of the APB is about four lattice constants and depends only weakly on the angle. Since the function $h(\phi)$ is negative at all angles, the linear APB structure is always stable.

8. Discussion

We have theoretically studied the properties of APBs in improper ferroelastics with tetragonal-to-orthorhombic phase transitions. The APBs were considered to be quasi-one dimensional and parallel to the tetragonal z axis but otherwise arbitrarily oriented. The expressions for the angular dependence of the free energy (23), the thickness (22) and the stresses (17) were derived in the framework of the phenomenological approach. The APB with the minimum free energy can be oriented at two angles ϕ_+ and $\phi_- = 90° - \phi_+$ given by the formulae in tables 1 and 2. If the quantity $A < 1$, then only the non-zero stress component in such an APB is σ_{zz}. If $A > 1$, the uniaxial inhomogeneous stresses σ_{zz} and $\sigma_{\eta\eta}$, which are parallel to the wall plane, must be imposed even around the APB with minimum energy to sustain its quasi-one-dimensional structure.

Using the free-energy expansion coefficients evaluated from experimental data it was shown that the linear boundary structure in Hg_2Br_2 is unstable for all APB orientations. In spite of this instability, which mainly depends on the coupling

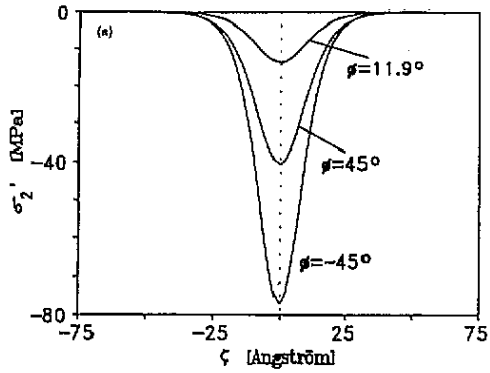

Figure 7. (*a*) The position-dependent stress component $\sigma_2'(\zeta)$ for three angles corresponding to extremal values of the free energy in KSCN. (*b*) The position-dependent stress component $\sigma_3'(\zeta)$ for three angles corresponding to extremal values of the free energy in KSCN. It depends only slightly on the angle.

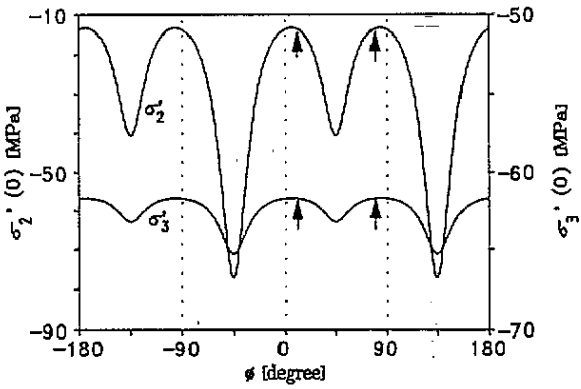

Figure 8. The stress components $\sigma_2'(0)$ and $\sigma_3'(0)$ versus ϕ in the centre of the APB. The APB has the minimum energy at 11.9° (78.1°) (shown by arrows in figure 6(*a*)). The component σ_2' (always non-zero) possesses its lowest magnitude at the angles 6° (or 84°); see also figures 3(*a*) and 4 for comparison.

coefficient $(\gamma' - \beta')/2$ between the order parameter components p and q (table 3) [23,27], we have calculated the angle-dependent properties of the analytically tractable linear APB structure. The boundary with the minimum free energy is tilted through about 15° (or about 75°) with respect to the FDW and the stress component σ_2' ($\equiv \sigma_{\eta\eta}$) becomes zero.

In KSCN the linear APB is stable for all orientations. Contrary to Hg_2Br_2 the stress component σ_2' is non-zero even in the APB with the minimum free energy tilted

through about 12° (or about 78°) with respect to the FDW. The magnitude of σ_2' near the transition temperature varies between 13 and 77 MPa and the stress σ_3' is about 60 MPa. It is interesting to compare the increase in the free energy due to the inhomogeneous strains in the APBs. In Hg_2Br_2 it represents from 0% to 42% of the total free energy, depending on the APB orientation. In KSCN it is 55% even for the APB with the minimum free energy. These ratios are temperature independent, contrary to the values of the free energy and of the stresses. From the angular dependence of the free energy in figure 2(*a*), one expects the orientations of the APBs in the interval (0°, 90°). This is in agreement with experiment [31,35].

Note that we have assumed that $g_a \ll g_i$ in both materials under consideration. Nevertheless, the coefficient g_a has not been determined from experiment up to now and its non-zero value could modify our numerical results to some extent. The properties of the APBs without the assumption of the quasi-one-dimensional structure of the wall remain also an open question.

Acknowledgments

The authors are grateful for fruitful discussions with Dr F Kroupa and they thank Professor H Warhanek for careful reading of the manuscript. The present work was supported by the Österreichischen Fonds zur Förderung der wissenschaftlichen Forschung unter Project P 8285. One of the authors (IR) is grateful to the Bundesministerium für Wissenschaft und Forschung for financial support.

References

[1] Sapriel J 1975 *Phys. Rev.* B **12** 11, 5128
[2] Janovec V 1981 *Ferroelectrics* **35** 105
[3] Zhirnov V A 1958 *Zh. Eksp. Teor. Fiz.* **35** 1175 (Engl. Transl. 1959 *Sov. Phys.–JETP* **35** 822)
[4] Bulaevskii L N and Ginzburg V L 1963 *Zh. Eksp. Teor. Fiz.* **45** 772 (Engl. Transl. 1964 *Sov. Phys.–JETP* **18** 530)
[5] Cao W and Barsch G R 1990 *Phys. Rev.* B **41** 4334
[6] Cao W, Barsch G R and Krumhansl J A 1990 *Phys. Rev.* B **42** 6396
[7] Lines M E and Glass A M 1977 *Principles and Applications of Ferroelectrics and Related Materials* ed W Marshall and D H Wilkinson (Oxford: Clarendon)
[8] Dvorak V and Janovec V 1965 *Japan. J. Appl. Phys.* **4** 400
[9] Fousek J 1967 *Japan. J. Appl. Phys.* **6** 950
[10] Rychetsky I 1991 *J. Phys.: Condens. Matter* **3** 7117
[11] Meleshina V A, Indenbom V L, Bagdasarov Kh S and Polkhovskaya T M 1973 *Kristallografiya* **18** 1218 (Engl. Transl. 1974 *Sov. Phys.–Crystallogr.* **18** 764)
[12] Barkley J R and Jeitschko W 1973 *J. Appl. Phys.* **44** 938
[13] Fouskova A and Fousek J 1975 *Phys. Status Solidi* a **32** 213
[14] Ishibashi Y and Dvorak V 1976 *J. Phys. Soc. Japan* **41** 1650
[15] Lajzerowicz J and Niez J J 1979 *J. Physique Lett.* **40** L-165
[16] Bogdanov A N, Telepa V T, Shatskÿ P P and Yablonskij D A 1986 *Zh. Eksp. Teor. Fiz.* **90** 1738
[17] Magyari E and Thomas H 1984 *Phys. Lett.* **100A** 11
[18] Gehring G A and Wragg M J 1987 *J. Phys. C: Solid State Phys.* **20** 3401
[19] Sonin E B and Tagancev A K 1989 *Ferroelectrics* **98** 291
[20] Bullbich A A and Gufan Yu M 1989 *Ferroelectrics* **98** 277
[21] Barta C, Kaplyanskÿ A A, Kulakov B B, Malkin B Z and Markov Yu F 1976 *Zh. Eksp. Teor. Fiz.* **70** 1429 (Engl. Transl. 1976 *Sov. Phys.–JETP* **43** 744)
[22] Rieder G 1959 *Abhandl. Braunschweigischen Wiss. Ges.* **11** 20
[23] Lemanov V V, Esayan S Kh and Chapelle J P 1981 *Sov. Phys.–Solid State* **23** 146

[24] Barta C, Zadokhin B S, Kaplyanskŷ A A, Malkin B Z, Markov Yu F, Morozova O V and Savchenko B A 1979 *Sov. Phys.–Crystallogr.* **24** 608
[25] Rychetsky I, Zikmund Z and Janovec V 1990 *Proc. 2nd Int. Symp. on Univalent Mercury Halides* ed K A McCarthy, C Barta and C Barta Jr (Prague: Institute of Physics, Czechoslovak Academy of Sciences) pp 143–6
[26] Barta C, Silvestrova I M, Pisarevskij Yu V, Moiseeva N A and Beljaev I M 1977 *Krist. Tech.* **12** 987
[27] Rychetsky I and Schranz W 1992 *Ferroelectrics* at press
[28] Yamamoto S, Sakuno M and Shimaka Y 1987 *J. Phys. Soc. Japan* **56** 4393
[29] Schranz W, Warhanek H and Zielinski P 1989 *J. Phys. C: Solid State Phys.* **1** 1141
[30] Janovec V, Schranz W, Warhanek H and Zikmund Z 1989 *Ferroelectrics* **98** 171
[31] Schranz W, Streuselberger T, Fuith A, Warhanek H and Götzinger M 1988 *Ferroelectrics* **88** 136
[32] Schranz W, Warhanek H, Blinc R and Zeks B 1989 *Phys. Rev.* B **40** 7141
[33] Schranz W, Streuselberger T, Fuith A and Warhanek H 1989 unpublished
[34] Blaschko O, Schwarz W, Schranz W and Fuith A 1991 *Ferroelectrics* **124** 139
[35] Schranz W and Rychetsky I 1993 to be published